



Slide burnishing—review and prospects

J. T. Maximov¹ · G. V. Duncheva¹ · A. P. Anchev¹ · M. D. Ichkova

Received: 8 March 2019 / Accepted: 16 May 2019 / Published online: 10 June 2019
© Springer-Verlag London Ltd., part of Springer Nature 2019

Abstract

This review paper is devoted to the slide burnishing (SB) of metal components—state-of-the-art, achievements and perspectives. SB belongs to the group of static methods for mechanical surface treatment used largely in aerospace, automotive and other industries. By means of the plastic deformation of the surface layers, the surface integrity (SI) of the respective component is improved greatly in terms of minimum roughness, micro-hardness and introduced residual compressive stresses. As a result, fatigue crack resistance, crack corrosion resistance, wear resistance and corrosion resistance increase dramatically. The main feature of SB is the sliding friction contact between the deforming element and the surface being treated. Using the differential-morphological method, an integrated classification of the static methods is created and the area of SB is outlined. The proposed morphological matrix, which can be expanded and supplemented contains existing burnishing methods as well as combinations of elements and interactions that can be used to synthesize new burnishing methods and tools. In addition, a literature review of the publications devoted to SB has been conducted. Further, an analysis of the published studies on different criteria has been carried out and graphic visualizations of the statistical results have been made. On this basis, relevant conclusions have been made and the directions for future investigations of SB have been outlined.

Keywords Mechanical surface treatment · Slide burnishing · Slide diamond burnishing · Diamond burnishing

List of symbols

f	Feed rate
F_b	Burnishing force
k	Number of the supporting balls
n	Number of passes
N	Number of cycles to failure
r	Deforming element radius
R_a	Surface roughness
v	Burnishing velocity
μ	Sliding friction coefficient
ω_w	Workpiece angular velocity
ω_r	Roller angular velocity

MST	Mechanical surface treatment
OP	Operational properties
PCD	Polycrystalline diamond
SB	Slide burnishing
SDB	Slide diamond burnishing
SHT	Surface heat treatment
SI	Surface integrity
SMB	Spherical motion burnishing
TCD	Thermochemical diffusion

Abbreviations

CNC	Computer numerical control
DB	Diamond burnishing
DMM	Differential-morphological method
FEM	Finite element method

✉ J. T. Maximov
jordanmaximov@abv.bg

¹ Department of Applied Mechanics, Technical University of Gabrovo, 5300 Gabrovo, Bulgaria

1 Introduction

Way back in 1920, the British scientist Griffith concluded that the inadequate strength of an isotropic solid body is due to the impaired continuity of the material (defects), with the general sizes of the gaps exceeding the intermolecular distances present in the material [1]. According to Griffith, the effective strength of construction materials would be 10 to 20 times higher if the defects were eliminated. However, these defects cannot be eliminated at this stage in the development of the science. They are introduced both in the process of obtaining the workpieces (metallurgical defects) and in the production process for the details from the respective workpieces. The

defects in the surface layer of the machine parts and structural components are particularly dangerous. It is well known that the surface layer is loaded most heavily during exploitation; it comes into contact with the surfaces of other components and is subjected to ambient impacts. Accordingly, the state of the surface layer in terms of its microstructure, residual stresses, and its depth of distribution, microhardness and roughness is crucial for the fatigue strength and life of the corresponding component. The control of these properties during the process of surface layer formation is the main reason for increased resistance to fatigue failure. The complex set of surface layer qualities is known as the surface integrity. Increasing the fatigue strength of the component requires a relevant technology for treating the surface layers, whereby the required set of properties for these layers is achieved: grain refinement microstructure, residual compressive stress, maximum depth of the compressive zone, increased microhardness and minimum roughness.

The residual stresses introduced by cutting are usually tensile in nature [2]. Moreover, the cutting is accompanied by the local destruction of the surface layers: For plastic materials, this destruction is preceded by significant plastic strains; for brittle material, a typical brittle destruction is observed. Therefore, the surfaces processed by cutting contain a plurality of micro-defects (dislocations) in the polycrystals within their microstructures. This plurality of dislocation configurations results in micro-cracks due to plastic deformations at the micro level and large micro-stresses. Upon the impact of an external load, these micro-cracks converge, and a single fatigue macro-crack with a relative size of 100 μm is formed. When the load is static, equalization of the stresses in the adjacent grains (stress redistribution) occurs, and the destruction is of the tough plastic type due to the increasing static load. When the stresses are variable, such equalization does not occur, and the macro-crack grows until the complete destruction of the respective component occurs. This process is very dangerous because the reduction in the cross section of the elements is not visible from the outside. Fatigue destruction is the most brittle destruction of the material under the given conditions. It should be noted that some cutting conditions provide residual compressive stresses in the machined layer and thus a longer fatigue life for the machined components can be obtained [3]. Actually, the plastic deformation behaviour of the surface layers of metal component is also observed in other mechanical treatments such as high-efficiency and heavy-load grinding of aerospace difficult-to-cut metallic materials: nickel-based superalloys [4–6], titanium matrix composites [7] and Ti_2AlNb intermetallics [8].

To improve the fatigue and tribological behaviour as well as the corrosion resistance of structural components, it is necessary to modify the set of topographic, mechanical, chemical

and metallurgical properties comprising the surface integrity (SI), of their surface layers. Surface engineering processes are used to modify the SI. They differ according to their corresponding impacts and consist of the mechanical surface treatment (MST) process (no alteration in the chemical composition), surface heat treatment (SHT) process (annealing, hardening, tempering), thermochemical diffusion (TMD) process (carburising, carbonitriding, nitriding) and combinations of these three processes. On the one hand, the SHT and TCD processes are costly, time-consuming and non-ecological, and, on the other hand, these processes are not sufficiently effective with respect to the fatigue behaviour of the metal components. Thus, SHT and TCD are used primarily to increase the hardness and wear resistance of the surface layers. In order to prevent destruction via fatigue effectively, the surface layers must be modified to decrease roughness, increase micro-hardness, increase residual compressive stresses and produce a refined microstructure; all of which can be accomplished in a cost-effective manner through MST.

The essence of MST is the plastic deformation of the surface peaks created by the sliding friction or rolling contact between a deforming element and the surface being treated. The peaks of the relief are plastically deformed, as the metal flows to the free valleys. As a result, the material undergoes strain hardening. At the same time, the contact between the deforming element and the surface being treated increases, the stresses decrease and the metal increases its resistance against further deformation. Thus, the plastic deformation is terminated at a certain depth below the surface, and the deformations are elastic only below this level. Due to differential material hardening, it is never possible to fill the valleys completely. The greater the tendency of a metal to harden, the less the valleys will fill and vice versa—for metals with plasticity close to the ideal value of one, maximal filling of the valleys is observed. The plastically deformed layer of the metal increases its volume. After termination of the contact with the deforming element, the elastically deformed, lower-lying layers seek to regain their original condition. The plastically deformed surface and subsurface layers that have increased their volume due to yielding to the deformation oppose this aspiration. Thus, the surface and subsurface layers are ‘pressed’ and the lower layers are ‘stretched’. In other words, useful residual compressive stresses are introduced into the surface and sub-surface layers, resulting in the increased fatigue strength of the treated material. At the same time, the deformed surface layers have increased micro-hardness and wear resistance.

Compared with finishing machining methods, MST has the following advantages:

- Greater productivity
- The material’s fibre integrity is stored
- Abrasive particles are missing on the treated surface

- There is less heating of the treated surface
- The roughness relief and its parameters have a more favourable effect on the operational properties of the surface
- The microstructure and hardening are more uniform, as the hardening is at a greater depth
- The residual stresses in the surface and the sub-surface layers are compressive

The methods used to implement MST are of two types: dynamic and static. An advantage of dynamic methods (such as shot peening, laser peening, water cavitation peening) is that they can be applied to the processing of complex surfaces without limitation. Chronologically, the dynamic methods precede the static methods. In 1871, Tilgham invented the sand blast process, which was the precursor of present-day shot peening [9]. The static methods are suitable for treating rotational surfaces. These static methods are known under the common name burnishing methods. One of the first patents involving these methods was published in 1916 [10]. In any static methods, the deforming element (or elements) is (1) a roller or ball, when the contact with the surface being treated is a rolling contact (in the case of a hydrostatic sphere [11], the sphere rotates around a instantaneous axis of rotation according to the Smallest Resistance Law); (2) spherical or cylindrical when the contact with the surface being treated is a sliding friction contact; (3) a ball whose contact with the surface being treated can be rolling contact at some moments in time and sliding friction in others; or (4) a roller whose contact with the surface being treated is both rolling and sliding friction contact.

In 1929, Föppl established the correlation between MST and the increased fatigue strength of the treated specimens for the first time [12]. In the 1930s, Thum studied the relation of roller burnishing with fatigue strength, corrosion fatigue and fretting fatigue [12]. As a result of the improved SI through MST, the fatigue strength of the respective structural component was increased significantly. The surveys of the burnishing methods' effects on fatigue strength continue to this day [13–15]. Many researchers have demonstrated experimentally that the MST increases surface wear resistance [16–23]. It has also been proven experimentally that MST increases the corrosion resistance of treated surfaces [24, 25].

An analysis of the literature on burnishing methods shows that there is no consensus among researchers on a number of concepts. For instance, the 'roller/ball' (burnishing) term is often used in the literature; it refers to the deforming element's shape and does not take the type of contact into account. Yet, even diamond burnishing, carried out via a spherically ended deforming diamond, is included in the ball-burnishing category, which is very confusing. Even when the shape of the deforming element is the same, if the contact is different

(rolling, sliding, respectively), different processes will be realized, and, as a result the SIs will have different indicators.

Often, in the literature, the same concept (for example, roller burnishing) is mentioned as a method and then as a process. For example, on the one hand, there is a roller-burnishing method, and, on the other hand, there is Ecoroll's roller-burnishing process. Of course, this concept can be used as both a method and a process, but such usage must be consistent with the meaning of the corresponding ratiocination. A burnishing method is a coherent time-space arrangement of two bodies (a deforming component and a treated surface) in the mechanical sense, with defined geometry, physical and chemical properties. Further, a burnishing process is an energy and mass exchange resulting from the coherent interaction between two bodies with clearly defined quantitative characteristics. Using the same method, but with different quantitative parameters, many deforming processes can be realized, and, as a result, the processed components will have, for example, different fatigue behaviours.

Slide burnishing (SB) is a static MST method. The method is implemented with simple devices and tools, which is its main advantage. SB is the common name for burnishing, which is implemented via sliding friction contact. When the deforming element is made of diamond (artificial or natural), the method is referred to as diamond burnishing (DB) or slide diamond burnishing (SDB). General Electric first introduced DB in 1962 in order to improve the SI of the treated components [26].

The purpose of this article is to create a united classification system for the static MST methods, i.e. burnishing methods and, on this basis, to outline the place, role and significance of SB within this system, review of the state of SB, and outline the prospects for its development.

2 Classification of burnishing methods

Classifications depending on the various burnishing method signs are known:

1. Depending on the shape of the deforming element, i.e. roller or ball: roller burnishing (Fig. 1) or ball burnishing

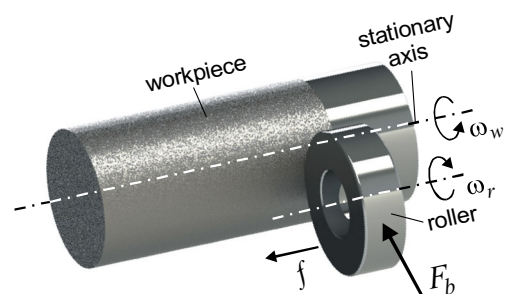


Fig. 1 Scheme of single roller burnishing

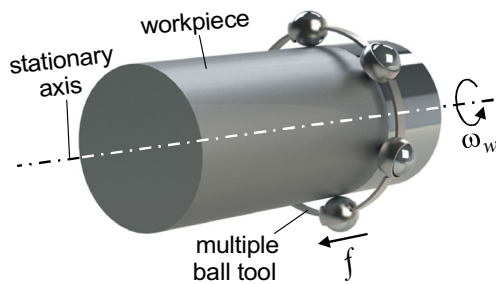


Fig. 2 Scheme of multiple ball burnishing

(Fig. 2), respectively. Obviously, classification under this sign is incomplete, as, for example, conducting SB with a cylindrical-ended deforming element (Fig. 3a) cannot fit into this classification. The classification under this sign is inadequate in terms of method of contact as well. For instance, both SB conducted through a spherical-ended deforming diamond (Fig. 3b) and burnishing with a hydrostatic sphere (Fig. 4) are classified as ball burnishing, regardless of their different contact methods (sliding friction versus rolling friction), which is the reason why different SIs are obtained. The misunderstandings can be minimized if the concept ‘ball burnishing’ is considered to ball burnishing with a hydrostatic sphere (rolling contact), while the first method given in the last example is completely recognizable under the SDB (or DB) name.

2. Depending on the type of the contact between the deforming element (roller or ball) and the surface being treated: (a) When the deforming element performs clean (without slipping) rolling with respect to the surface being treated, then the contact is rolling friction and the methods are, respectively, roller/ball burnishing; (b) if the contact is sliding friction, the method is SB.
3. Depending on the desired SI. Ecoroll uses the terms ‘roller burnishing’ and ‘deep rolling’ processes [11]. The main objective of the first is to produce smoothing, wherein the roughness is reduced considerably. The other attributes of the surface layer (increased micro-hardness, compressive residual stresses) inherent in the MST also exist but are rather concomitant and not significant. Deep rolling aims to produce three effects simultaneously: burnishing, cold

work and compressive residual stresses with maximum magnitude in absolute value and of considerable depth. Lambda Research invented the low-plasticity burnishing process [27–30], which was intended to create a compressive zone with large absolute values of the residual stresses at great depth, whereby the magnitude of the equivalent plastic strain (cold work) is automatically controlled in order not to exceed the set limit. This control ensures the performance of the structural components that are subjected to overloading or high temperatures. In fact, the first Ecoroll process is implemented through the roller burnishing method. Deep rolling and low-plasticity burnishing processes are conducted by one and the same method—ball burnishing with a hydrostatic sphere. Obviously, different quantitative values of the characteristics of a given method lead to the realization of different processes. As can be seen, there is no universal classification of the burnishing methods. The differential-morphological method (DMM) allows not only a universal classification of the existing burnishing methods using a variety of signs but also of the new burnishing methods and tools to be synthesized. Y. N. Kuznetsov developed DMM [31] based on the morphological method proposed by the Swiss astronomer Fritz Zwicky [32]. In the present study, DMM is used for the classification and synthesis of burnishing methods. The method is ‘open’, i.e. the morphological signs of the object can always be expanded with new features according to the researcher’s preferences. The structure of the generalized burnishing method, shown in Fig. 5, consists of the following elements: 1, workpiece element; 2, deforming element; and 3 and 4, the elastic and viscous elements, respectively, for setting the burnishing force. For each element, the signs and the sub-signs can be defined in arbitrary order.

Table 1 contains the morphological signs and sub-signs to the second order for the elements in Fig. 5. On the basis of the morphological sub-signs from second order, the so-called morphological matrix has been arranged:

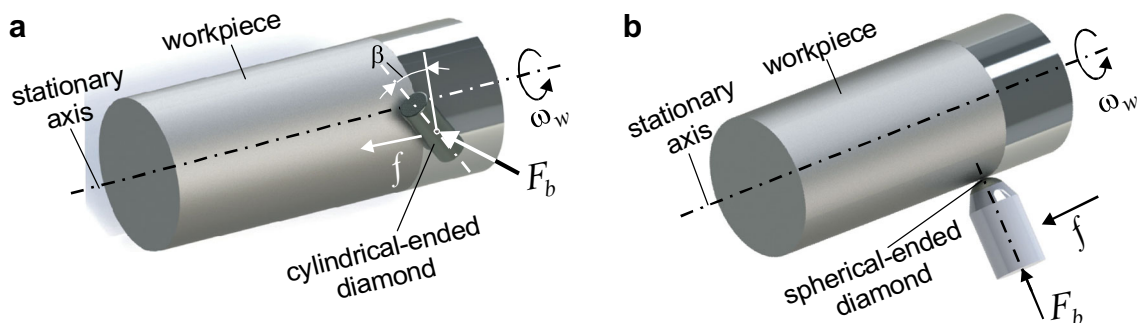


Fig. 3 Scheme of slide burnishing **a** with cylindrical-ended tool and **b** with spherical-ended tool

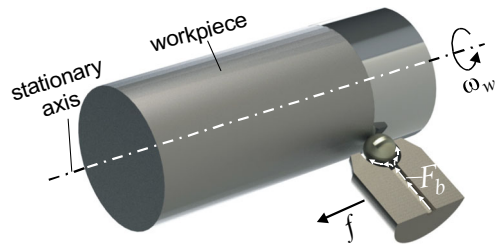


Fig. 4 Ball burnishing with a hydrostatic sphere

$$[M] = \begin{bmatrix} 1.1.1 & 1.2.1 & 2.1.1 & 2.2.1 & 2.3.1 & 3.1.1 & 3.2.1 & 4.1.1 & 5.1.1 \\ 1.1.2 & 1.2.2 & 2.1.2 & 2.2.2 & 2.3.2 & 3.1.2 & 3.2.2 & 4.1.2 & 5.1.2 \\ 1.1.3 & 1.2.3 & 2.1.3 & 2.2.3 & 2.3.3 & 0 & 3.2.3 & 0 & 5.1.3 \\ 1.1.4 & 1.2.4 & 2.1.4 & 2.2.4 & 2.3.4 & 0 & 3.2.4 & 0 & 5.2.1 \\ 1.1.5 & 1.2.5 & 2.1.5 & 2.2.5 & 2.3.5 & 0 & 0 & 0 & 5.2.2 \\ 1.1.6 & 1.2.6 & 2.1.6 & 0 & 2.3.6 & 0 & 0 & 0 & 0 \\ 0 & 1.2.7 & 0 & 0 & 2.3.7 & 0 & 0 & 0 & 0 \end{bmatrix}$$

The matrix contains the last column of Table 1. Therefore, the number of columns of the matrix should be equal to the number of morphological signs. In the given example, the number of columns is smaller by one unit, because the combinations of sub-signs of 5.1 on one side and of 5.2 on the other hand are incompatible.

In order to synthesize a burnishing method, it is necessary to make a combination containing one element (with a number other than zero) from each column. Each element of the first column is combined with one element from the other columns. Each (compatible) combination corresponds to one burnishing method. Of course, there are also incompatible combinations. For example, some of the known methods are a combination of the following:

- [1.1.1 1.2.3 2.1.1 2.2.5 2.3.6 3.1.2 3.2.4 4.1.1 5.2.2] corresponds to the ball burnishing with a hydrostatic sphere of the outer cylindrical surfaces (see Fig. 4).
- [1.1.1 1.2.3 2.1.2 2.2.4 2.3.5 3.1.1 3.2.1 4.1.2 5.1.1] corresponds to the roller burnishing of the outer cylindrical surfaces (see Fig. 1).
- [1.1.2 1.2.3 2.1.1 2.2.2 2.3.2 3.1.1 3.2.1 4.1.2 5.1.1] corresponds to the SDB with spherical-ended tool of the holes.
- [1.1.1 1.2.3 2.1.2 2.2.2 2.3.2 3.1.1 3.2.1 4.1.2 5.1.3] corresponds to the SDB with a cylindrical-ended tool of the outer cylindrical surfaces (see Fig. 3a).

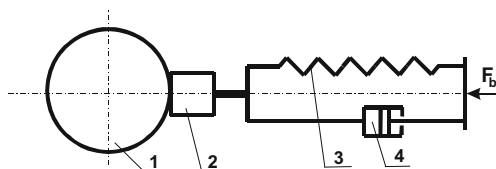


Fig. 5 Structure of generalized burnishing method: 1 workpiece; 2 deforming element; 3 and 4 elements, respectively elastic and viscous, for setting burnishing force

Table 1 Differential-morphological table

Elements of the structure	Morphological signs	Morphological sub-signs
1. Workpiece	1.1. Geometrical form	1.1.1. External cylindrical surface
		1.1.2. Internal cylindrical surface
		1.1.3. Flat surface
		1.1.4. Complex surface
		1.1.5. Outer conical surface
		1.1.6. Inner conical surface
	1.2. Motion	1.2.1. Motionless
		1.2.2. Translation
		1.2.3. Rotation around a stationary axis
		1.2.4. Rotation around a momentary axis of rotation
		1.2.5. Superposition of translation and rotation around a stationary axis (planar motion)
		1.2.6. Superposition of translation and rotation around a momentary axis of rotation
2. Deforming element	2.1. Geometrical form	1.2.7. Undefined
		2.1.1. Outer spherical
		2.1.2. Outer cylindrical
		2.1.3. Plane
		2.1.4. Internal toroidal
		2.1.5. External toroidal
	2.2. Material	2.1.6. Complex surface
		2.2.1. Natural diamond
		2.2.2. Artificial diamond
		2.2.3. Sintered carbide
		2.2.4. Hardened tool steel
		2.2.5. Ceramic
2.3. Motion	2.3.1. Motionless	
	2.3.2. Translation	
	2.3.3. Rotation around a stationary axis	
	2.3.4. Rotation around a momentary axis of rotation	
	2.3.5. Superposition of translation and rotation around a stationary axis (planar motion)	
	2.3.6. Superposition of translation and rotation around a momentary axis of rotation	
	2.3.7. Undefined	
3. Elastic element	3.1.1. Exists	

Table 1 (continued)

Elements of the structure	Morphological signs	Morphological sub-signs
	3.1. Availability	3.1.2. Does not exist
	3.2. Physical nature	3.2.1. Tension–compression
		3.2.2. Torsion
		3.2.3. Bending
		3.2.4. Does not work
4. Viscous element	4.1. Availability	4.1.1. Exists
		4.1.2. Does not exist
5. Mutual disposition of the axes of the workpiece and the deforming element	5.1. Fixed	5.1.1. Parallel
		5.1.2. Intersecting (coplanar)
		5.1.3. Crossed (do not lie in one plane)
	5.2. Changing	5.2.1. According to a given law
		5.2.2. Random

- [1.1.1 1.2.3 2.1.5 2.2.4 2.3.5 3.1.2 3.2.4 4.1.2 5.1.2] corresponds to the spherical motion burnishing (SMB) of the shafts (Fig. 6a).
- [1.1.2 1.2.1 2.1.1 2.2.4 2.3.6 3.1.2 3.2.4 4.1.2 5.1.2] corresponds to the SMB of the holes (Fig. 6b) and so on.

The method implemented with a deforming ball with undefined motion occupies an intermediate position between SB and ball burnishing. This method is implemented with devices in which the deforming ball is supported by other balls or a rigid plane surface (Fig. 7) [33–40]. For a given burnishing device construction (a given support configuration), the type of contact between the deforming ball and the treated surface (rolling friction or sliding friction) depends on the friction coefficients between the deforming ball and the surface being

burnishing, on the one hand, and between the deforming ball and the supports, on the other hand. This method is defined by the following combination:

[1.1.1 1.2.3 2.1.1 2.2.4 2.3.7 3.1.2 3.2.4 4.1.2 5.2.2]

A burnishing method (Fig. 8) that achieves rolling and sliding effects simultaneously on the burnishing point of the workpiece is also known [41, 42]. The aim of the method is to accomplish a finish with superior SI. This method is defined by the following combination:

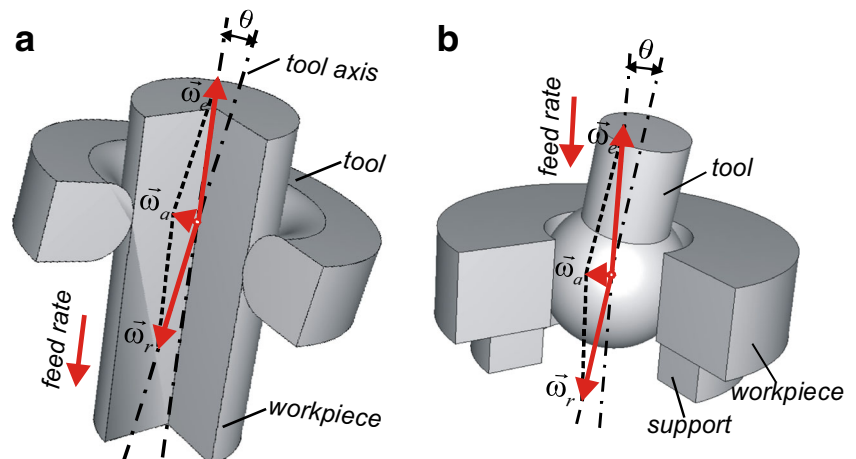
[1.1.1 1.2.3 2.1.2 2.2.4 2.3.5 3.1.1 3.2.1 4.1.2 5.1.3]

The proposed morphological matrix, which can be expanded and supplemented, contains not only the existing burnishing methods, but it also contains combinations that can be the basis for the synthesis of new burnishing methods and burnishing tools.

3 Essence of SB

The most important feature of SB is the sliding friction contact between the deforming element and the surface being treated. SB is kinematically similar to turning but, instead of a cutting tool blade, a spherical-ended (most frequently) or cylindrical-ended deforming element is moved under pressure over the work surface, causing plastic deformation on the surface and subsurface layers (Fig. 9). SB is especially suited for shafts and large bores but can be implemented on flat-face surfaces, as well. The method can be implemented in one of two ways: (1) The deforming element can be pressed elastically against the surface being treated (as shown in Fig. 9), and (2) without the aid of an elastic element (rigid fixing). The second variant is applied to short-length surfaces, where the shape accuracy is improved by one or two classes. When the deforming element is supported elastically, the shape accuracy is not improved—such improvement must be ensured via pre-treatment. The basic governing factors of the SB process are the sphere radius of the deforming element r , mm , burnishing force F_b , N , feed

Fig. 6 Scheme of spherical motion burnishing **a** of shafts and **b** of holes



rate f , mm/rev , and burnishing velocity v , m/min . The number of passes, working scheme and lubricant used are additional factors. SB devices and tools are compatible with every conventional and CNC-controlled lathe or CNC turning centre. Therefore, a workpiece can be slide burnished in one setting directly after machining. The deforming element is most often a diamond—usually a polycrystalline synthetic diamond. The deforming element may also be made of sintered carbide or hardened tool steel. A diamond deforming element has the following advantages: high hardness, high wear resistance (abrasive and adhesive), high compressive strength and a low friction sliding coefficient. Since SB is conducted under sliding friction conditions, the above properties protect the treated material from temperature overloading, enable the SB of the hardest steels and alloys, and prolong the lifetime of the deforming tool. SB is a very economical method for producing mirror-like surface finishes on a wide range of ferrous and nonferrous machined surfaces. Since set up and operation is relatively simple and cycle times are short, no special operator skills are required.

4 Literary survey of SB and discussion

As noted in Sect. 1, General Electric invented SDB in the middle of the last century. A little later, the method spread to the machinery industry in the former Soviet Union, resulting in a massive number of studies performed by Russian researchers in the third quarter of the last century. Hundreds of publications from this period were devoted to both the SI of diamond-burnished specimens and the study of the process physics: generated heat, wear on the deforming diamond during operation and properties of the lubricants. Quite a few publications of this period refer to the synthesis and study of the physical properties of synthetic diamonds. A

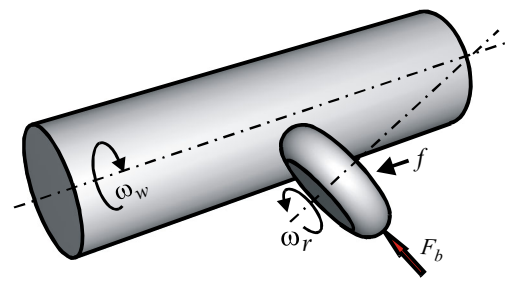


Fig. 8 Scheme of the burnishing that achieves simultaneously rolling and sliding effects

comparatively complete bibliographic reference for the Soviet researchers' publications from this period is contained in the famous book by Yatsenko et al. [43]. Since that time, researchers around the world have investigated the SB process extensively. In terms of modern researchers, Korzynski [44] has made a significant contribution to the development of SB. Additional research groups contributing to SB include CIT, Rzeszow, Poland [44–53]; IAMT, Cracow, Poland [54–57]; KSU, Kurgan, Russia [58]; ZNTU, Zaporozhe, Ukraine [59]; Aalto University, Espoo, Finland [60, 61]; Kecskemet College, Hungary [62, 63]; SMSE, China [64–67]; NITK, Surathkal, India [68–70]; and the Technical University of Gabrovo, Bulgaria [71–83]. Some experimental studies by other researchers have also been reported worldwide [84–119].

The investigations concerning SB can be classified according to several indicators, as shown in Table 2. Figure 10 shows that most publications are devoted to SI resulting from SB. The exploitation properties of the slide-burnished surfaces are significantly less studied. The physical nature of the process is studied least—only 5% of the publications are dedicated to this problem. The nature of SB differs from that of burnishing with a rolling contact (roller/ball burnishing). In SB, the tangential contact between the deforming element and the surface being treated is one of sliding friction. Regardless of the low

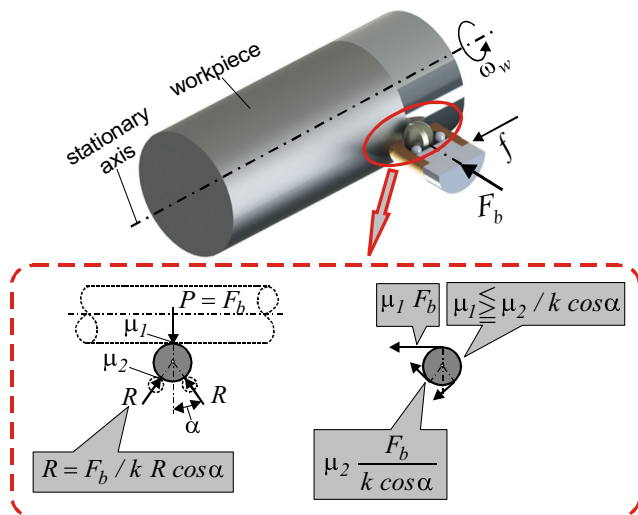


Fig. 7 Ball burnishing with undefined ball motion

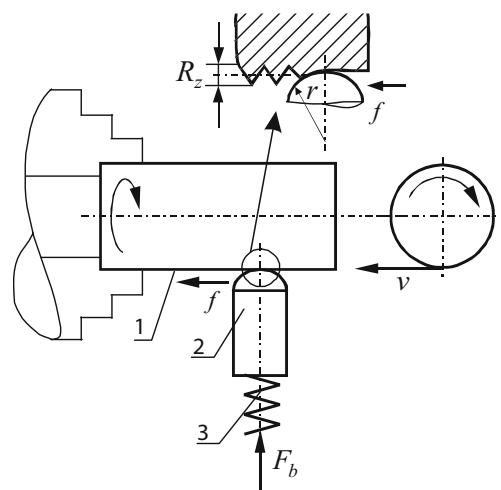


Fig. 9 Kinematics of SB

Table 2 Classification of the investigations on SB

Indicators	Subindicators	Reference
A. Subject of the study	A.1. SI of the slide burnished surface for specific material	
	A.1.1. Roughness	[48, 49, 52, 54, 55, 58–60, 62, 63, 66, 69–72, 74, 76, 77, 79–81, 85, 87, 89–92, 95–98, 100, 103, 105–107, 109, 110, 112–118]
	A.1.2. Surface topography	[46–50, 53, 57, 70, 90, 102, 117]
	A.1.3. Accuracy of the form	[60, 108]
	A.1.4. Waviness	[66]
	A.1.5. Microhardness	[48, 54, 55, 59, 60, 65, 68–70, 74, 79–81, 85, 88, 94, 95, 98, 104, 107, 110, 112–117]
	A.1.6. Residual stresses	[48, 49, 59, 60, 68, 70–72, 74–77, 79–83, 90, 94, 98, 99, 104, 108, 115, 119]
	A.1.7. Microstructure	[53–55, 58, 59, 69, 76, 77, 83, 88, 91, 93–95, 105, 106, 110, 113, 115, 117]
	A.2. Operational properties (OP) of slide burnished surfaces	
	A.2.1. Wear resistance	[55, 80, 84, 116]
	A.2.2. Corrosion resistance	[45, 95]
	A.2.3. Corrosion cracking resistance	[88]
	A.2.4. Fatigue behaviour	[48, 49, 71, 76, 77, 80, 83, 84, 101]
	A.2.5. Other (slow strain rate test; relative loss of fracture energy)	[88]
	A.3. Physical nature of the process	
	A.3.1. Life time of the deforming element	[86]
	A.3.2. Generated heat	[82]
	A.3.3. Friction coefficient	[78]
	A.3.4. Contact mechanism	[64]
	A.3.5. Energy-power parameters	[73, 79, 81]
	B. The effect of using a different material and geometrical form of the deforming element	B.1. Material of the deforming element
B.1.1. Diamond		[45–55, 57–59, 62–66, 68–71, 74–78, 80, 82, 83, 85, 86, 89, 90, 93, 99–106, 108–110, 113, 116–119]
B.1.2. Hardened tool steel		[81, 92, 97]
B.1.3. Sintered carbide		[60, 72, 73, 79, 87, 91, 94, 96–98]
B.2. Working surface of the deforming element		
B.2.1. Spherical		[45–47, 49–55, 57–60, 62, 63, 68–71, 74–78, 80–83, 85, 86, 88–100, 103–110, 112–119]
B.2.2. Cylindrical		[48, 64–66, 87, 101, 102]
B.2.3. Toroidal	[72, 73, 79]	
C. Method of the study	C.1. Analytical	[51, 52]
	C.2. FE analysis	[72]
	C.3. Analytical and experiment	[48, 53, 64, 73, 78, 79, 81, 96]
	C.4. FE analysis and experiment	[71, 74–76, 82, 107, 119]
	C.5. Experiment	[45–47, 49, 50, 54, 55, 57–60, 62, 63, 65, 66, 68–70, 77, 80, 83, 85, 86, 88–95, 97–102, 104–106, 108, 110, 112–115, 118]
D. Materials processed by SB	D.1. Steels	
	D.1.1. Unhardened	[45–49, 52, 59, 68–73, 75, 78–83, 87, 88, 90, 92, 94, 95, 97–101, 105, 116–118]
	D.1.2. Hardened	[53–55, 57, 58, 60, 62, 63, 102, 106, 110, 113]
	D.2. Cast iron	none
	D.3. Non-ferrous alloys	

Table 2 (continued)

Indicators	Subindicators	Reference
	D.3.1. 2024-T3 Al alloy	[74, 76, 77]
	D.3.2. Other aluminium alloys	[64–66, 93, 103, 104, 107–109, 114, 115]
	D.3.3. Aluminium composites	[85, 89, 113]
	D.3.4. Titanium alloys	[119]
	D.3.5. Magnesium alloys	[50, 112]
	D.3.6. Other non-ferrous metals and alloys	[65, 66, 91, 96]
E. Type of the surface treated	E.1. Outer cylindrical	[45–50, 52, 59, 60, 62–66, 68–70, 72–74, 76–80, 83, 85, 87–89, 93, 95, 98, 100–104, 106, 108, 110, 112–114, 116–119]
	E.2. Holes	[53, 71, 75, 81, 82, 92]
	E.3. Flat surfaces	[54, 55, 58, 90, 91, 94, 96, 97, 107, 115]
	E.4. Complex surfaces	[90]
	E.5. Discontinuous cylindrical surface	[105]
F. Comparison between SB and roller burnishing		[116]
G. Investigation of the SB process parameters	G.1. Radius of the spherical-ended tool r	[47, 50, 51, 66, 70, 71, 74–76, 78, 80, 89, 99, 100, 109, 117]
	G.2. Diameter of the cylindrical-ended tool d	[48, 100, 101]
	G.3. Burnishing force F_b	[47, 48, 50, 52, 57–59, 62, 63, 65, 69, 70, 74–76, 78, 80, 85, 87, 89, 90, 95–102, 104–106, 108, 110, 112–118]
	G.4. Burnishing depth a_p	[65–68]
	G.5. Feed rate f	[47, 48, 50, 51, 57, 59, 62, 63, 66, 67, 69–72, 74, 75, 78, 80, 83, 85, 87, 89, 90, 95–102, 104–106, 108–110, 112–119]
	G.6. Burnishing velocity v	[66, 67, 69, 70, 74, 78, 80, 87, 89, 90, 92, 95–101, 104, 109, 112, 115–118]
	G.7. Number of passes n	[58, 68, 70, 74, 77, 83, 96, 98, 108, 112, 114, 116, 117]
	G.8. Working scheme	[70, 74, 77]
	G.9. Lubricant	[68, 77, 87, 98]

friction coefficient obtained in the case of using a synthetic diamond as a deforming element, the friction forces work is significant and dissipates into heat. Therefore, the deforming process in SB has a thermo-mechanical nature and the heat generated is the reason thermoplastic deformations emerge. Thus, all of the major effects of SB (smoothing, cold work, introducing residual compressive stresses) depend on the heat

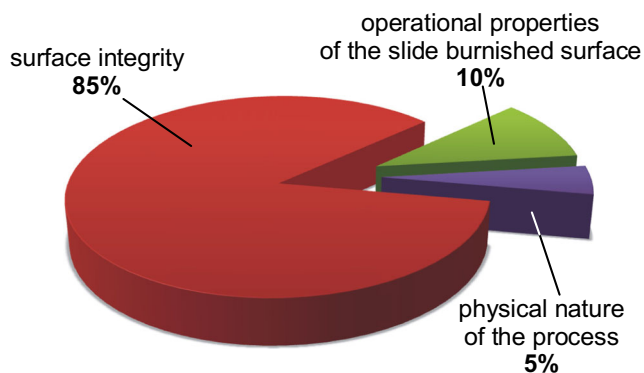


Fig. 10 Percentage share of the study objects

generated due to the softening effect of the surface layer. The temperature gradient in terms of the depth is very large—the

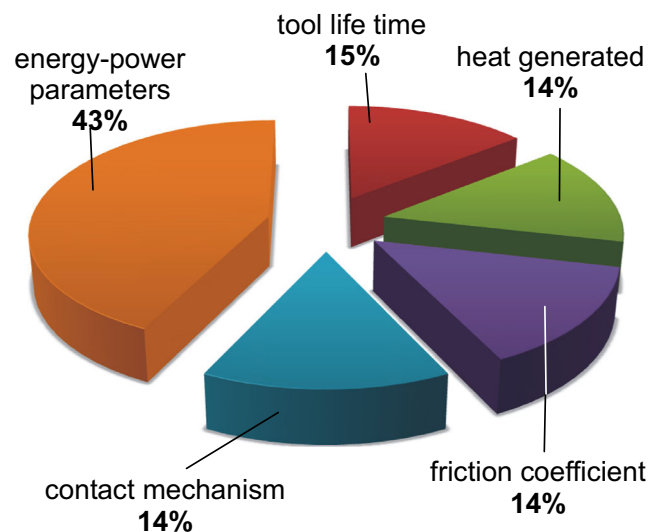


Fig. 11 Percentage share of the SB process physical nature

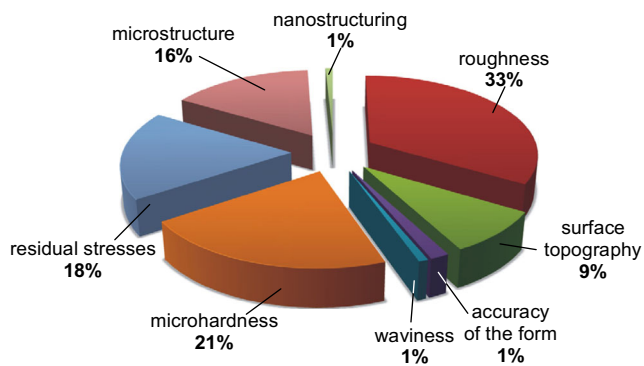


Fig. 12 Percentage share of the SI components

temperature decreases sharply with depth. When the ‘deforming element-workpiece’ system is fully determined via geometry and physical-mechanical properties, the generated heat depends on the burnishing force, the burnishing speed and the friction coefficient. Due to the very short impact time of the deforming element at a given point on the surface being treated, the very small contact area, and the very high temperature gradient, the experimental determination of the temperature is very difficult. The formation and redistribution of the residual stress field in real-time is practically impossible to determine with an experimental study. These difficulties can be overcome through a FEM simulation of the thermo-mechanical deforming process in SB. For example, a sliding friction coefficient was found in a single publication [78] for a particular combination of materials of the deforming element and the surface being treated. This friction coefficient is an important component in an adequate FE model of the SB, and its precise definition is a prerequisite for more reliable FE results. Thus, the lack of information on the sliding friction coefficient automatically limits the possibility of reliable FE analyses. Information on deforming element wear [86] and heat generated [82] due to friction is also scarce—only one publication is dedicated to the relevant problem (Fig. 11). The heat generated causes a reduction in the surface residual stresses, but this important problem is illuminated in only two publications [80, 82].

In terms of the SI elements, the greatest attention is paid to the roughness obtained (Fig. 12), followed by the

Table 3 Methods used for determination of the residual stresses

Methods	References
X-ray diffraction	[68, 70, 74, 76, 77, 79–81, 89, 90, 94, 98, 104, 108, 115]
Hole drilling	[60, 61, 119]
Split ring	[59, 75, 99]
Weisman-Phillips method	[48, 49]
FEM	[71, 72, 75, 76, 82, 119]

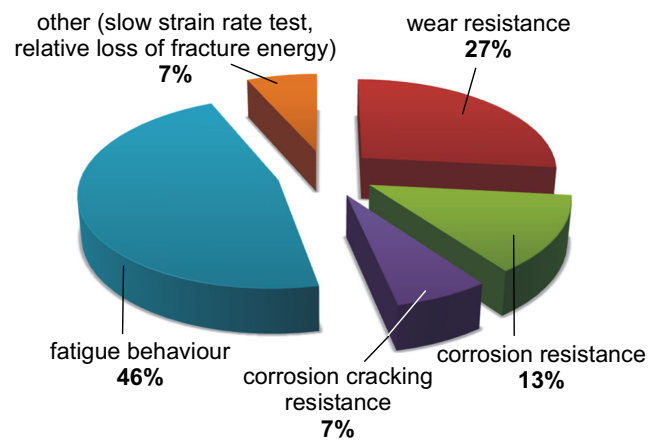


Fig. 13 Percentage share of the OP components

microhardness, residual stresses and microstructure of the surface layers. The methods used for the determination of the residual stresses are shown in Table 3. With six exceptions, experimental methods have been used (destructive and non-destructive), and non-destructive X-ray diffraction is the most commonly used method. The least-studied problem is related to the nanostructuring of the surface layers (see Fig. 12). However, this direction is promising because the nanostructured layers provide great micro-hardness, wear resistance and large low-cycle fatigue strength.

Figure 13 shows that the fatigue behaviour is the most commonly investigated operational property (OP), followed by wear resistance. The integral approach (through S-N curves) is most commonly used to study the fatigue behaviour, while very little attention is devoted to the mechanism of delaying the formation and propagation of fatigue macro-cracking. Corrosion cracking resistance has been studied least, but this is a current problem in engineering practice.

More than three quarters of the studies are devoted to SDB (Fig. 14), i.e. diamond deforming elements. Obviously, the application of a sintered carbide as a

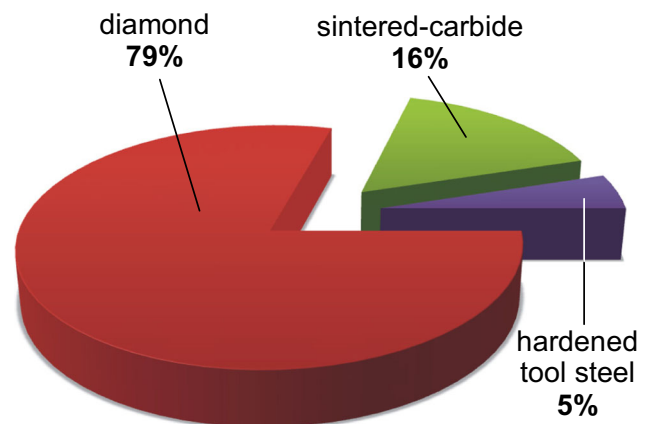


Fig. 14 Percentage share of the deforming element material

Table 4 Type of the diamond used

Kind of diamond	References
Synthetic polycrystalline diamond (PCD)	[45–47, 49–53, 56, 58, 62–66, 71, 75–78, 80, 82, 83, 90, 93, 102, 108, 109, 118, 119]
PCD with bonding phase of titanium silicon carbide ceramic (Ti ₃ SiC ₂)	[48, 54, 55, 57, 85, 101, 103, 110, 111, 113]
Not mentioned	[116, 117]
DB-200	[69, 70]
Synthetic diamond grade of ASB-1	[99, 100]
Single crystal diamond	[86, 89, 104–106]

deforming element is used considerably less, and the hardened steel is used least. Table 4 shows that the synthetic PCD is the most commonly used diamond. A single-crystal diamond is used considerably less. When considering the group of sintered carbides, the wolfram carbides are most often used (Table 5). The working surface of the deforming element (see Table 2) most often has a spherical form (84%). The effect of using a cylindrical shape is examined considerably less (11%). The toroidal form (5%) is applied only to the SMB of shafts.

Figure 15 shows that the purely experimental approach is preferred most by researchers (74%). The analytic + experiment and FE analysis + experiment combinations occupy, respectively, second and third places. The analytical and the FE approaches are rather exceptions. The impression is that FEM is used significantly less for SB analysis than for the analysis of roller/ball burnishing.

Considerably more research is devoted to SB of steels (65%) compared to SB of nonferrous materials (35%) of the studies (Fig. 16). Information about SB of cast iron is missing. The majority of the nonferrous materials investigated are aluminium alloys and aluminium composites. The impression is that SB of 2024-T3 Al alloy, titanium and magnesium alloys (typical for the aerospace industry) is relatively poorly studied. The probable reason for this

Table 5 Type of the sintered carbides used

Kind of sintered carbides	References
Sintered carbides	[84, 94]
Wolfram carbides	[60, 87, 96–98]
Ferrotic C	[72, 73, 79]
Diamond-like carbon-coated carbide	[91]
Silicon carbide	[97]

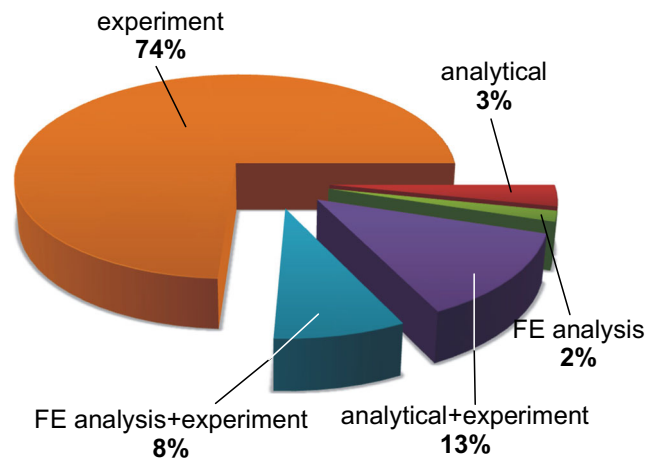


Fig. 15 Percentage share of the methods of study

neglect is the imposed belief that SB is only used for smoothing, i.e. that the application of SB is aimed primarily at obtaining mirror-like surfaces. On the other hand, the beneficial effect on the fatigue strength is associated largely with Ecoroll’s deep rolling process. In fact, SB has great potential in terms of the being able to create a zone with residual compressive stresses due to the small contact area between the deforming element and the surface being treated. The studies conducted in [76, 77] have shown that SB of 2024-T3 Al alloy not only provides roughness on the order of $R_a = 0.05 \mu m$ but also increases the fatigue life dramatically (hundreds of times). Moreover, the fatigue behaviour of the corresponding component can be controlled by appropriate selection of the SB process parameters. Therefore, SB can be implemented as mixed burnishing [120]. Tables 6 and 7 contain generalized information regarding the treated material—the specific type of material and results obtained for roughness, micro-hardness and residual stresses. It appears that full information exists only

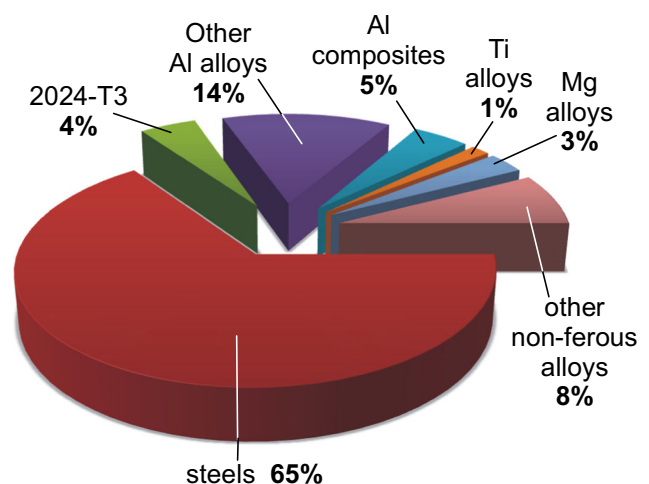


Fig. 16 Percentage share of the treated material

Table 6 Summary of SB of steels

Steel	R_a (μm)	Micro-hardness improvement (%)	Residual stresses				References
			Hoop (MPa)		Axial (MPa)		
			Surface	Max	Surface	Max	
Carbon steels							
Rb40	0.22	10.25	–	–	–	–	[116]
AISI 1045	0.27	16.8	–	–	–	–	[87, 95]
R260	0.27	–	–400	–600	–	–	[75]
steel 45	–	200	–1004	–1022	–847	–896	[94]
40HM	–	–	–	–	–	–	[101]
Low-alloy steels							
36CrNiMo6	0.3	44.03	–	–	–	–	[117]
AISI 4140	0.131	–	–	–	–	–	[118]
34CrNiMo6	0.08	11.21	–1200	–1400	–	–	[60, 61]
42Cr4Mo4	0.05	29	–275	–389	–	–	[48, 49, 52, 102]
41Cr4	0.073	73.91	–	–	–1130	–	[49]
20Cr4	0.18	–	–	–	–	–	[58]
100Cr6	0.15	–	–	–	–	–	[62, 63]
37Cr4	0.12	–	–100	–400	–	–	[71–73, 78, 79, 81–83]
FeC0.15Cr12Ni2	–	–	–100	–528	–	–	[99]
30XГCH2A-BД	0.068	–	–	–	–	–	[100]
Tool steels							
105V	–	–	–	–	–	–	[53]
100Cr	–	–	–	–	–	–	[53]
PDS5	0.067	–	–	–	–	–	[97]
Nitrided AISI D2	0.23	81.8	–	–	–	–	[54]
Sverker 21	0.23	57.75	–	–	–	–	[55, 56, 111]
Vanadius 6	0.24	79.10	–	–	–	–	[55, 56, 111]
X153CrMoV12	–	–	–	–	–	–	[57]
Stainless steels							
Kh12NMBF	0.2	38.38	–150	–428	–	–	[59]
X6CrNiMoTi17-12-2	–	26	–	–	–	–	[45]
317Ti	–	–	–	–	–	–	[46, 47]
X20Cr13	0.18	–	–	–	–	–	[58]
UR52N	–	63.63	–	–	–	–	[88]
AISI 316Ti	0.055	32.52	–400	–480	–800	–800	[80]
AISI 316	0.07	35.71	–300	–	–800	–	[90]
SKH57	0.055	–	–	–	–	–	[92]
17-4 PH	0.05	22.06	–310	–352	–	–	[68–70]
SUS420J2	0.025	5.88	–1047	–	–	–	[98]
SUS316	0.08	160	–700	–	–	–	[104]

for AISI 316Ti, while, for other materials, there is no information on the three characteristics.

Figure 17 shows that three-quarters of the studies are devoted to the SB of outer cylindrical surfaces, while the

SB of holes is covered by only 6% of the studies. It appears that the SB of planar surfaces makes up a significant share of these studies (16%), which somewhat disproves the opinion that SB ‘is also possible in terms

Table 7 Summary of SB of nonferrous materials

Nonferrous materials	R_a (μm)	Micro-hardness improvement (%)	Residual stresses				References
			Hoop (MPa)		Axial (MPa)		
			Surface	Max	Surface	Max	
2024-T3 Al alloy	0.06	50.4	–	–	–220	–220	[74, 76, 77]
Other aluminium alloys							
7075	0.08	71.43	–850	–	–	–	[104, 114]
1050A aluminium	0.68	7.3	–30	–	–30	–45	[115]
LY12	0.15	^a	–	–	–	–	[64–67]
Al-Zn-Mg	–	32	–	–	–	–	[93]
AlCu4MgSi(A)	0.19	–	–	–	–	–	[103]
6061-T6	0.108	93.14	–125	–217	–	–	[107]
Aluminium matrix composite							
AlMg1SiCu	0.15	30	–	–	–	–	[85]
A390+SiC	0.13	50	–	–	–	–	[85]
AA2124	0.04	–	–220	–	–380	–	[89]
Titanium alloy							
Ti-6Al-4V	–	–	–230	–460	–	–	[119]
Magnesium alloy							
AZ91D	0.43	^a	–	–	–	–	[112]
AZ91	–	–	–	–	–	–	[50]
Other non-ferrous alloy							
Brass H62	0.08	^a	–	–	–	–	[65, 66]
Ni-based alloy	0.1	33.1	–	–	–	–	[91]
Oxygen-free copper 101	0.183	–	–	–	–	–	[96]

^a There is no information about the initial micro-hardness

of treating flat and shaped surfaces, but it is not used in practice’ [44].

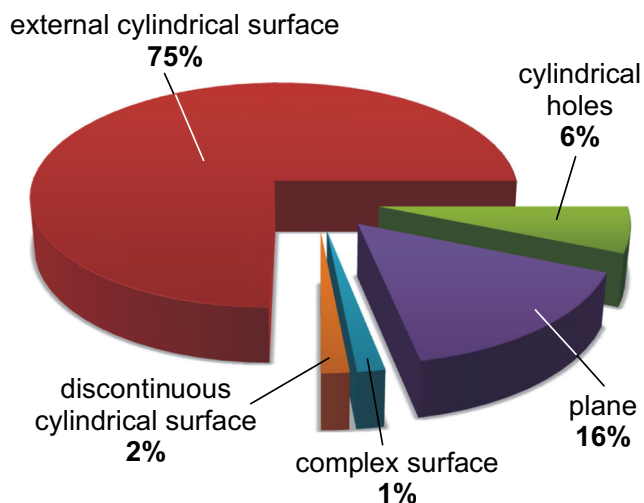


Fig. 17 Percentage share of the type of the treated surface

The percentage shares of the SB process parameters studied are shown in Fig. 18. The most commonly studied parameters are feed rate and burnishing force (which is directly correlated with the burnishing depth). The additional process parameters (lubricant used, number of passes and working schemes) have been studied considerably less. The importance of the additional parameters should not be underestimated, as they have a significant effect on the fatigue life of the slide-burnished components, as found in [77].

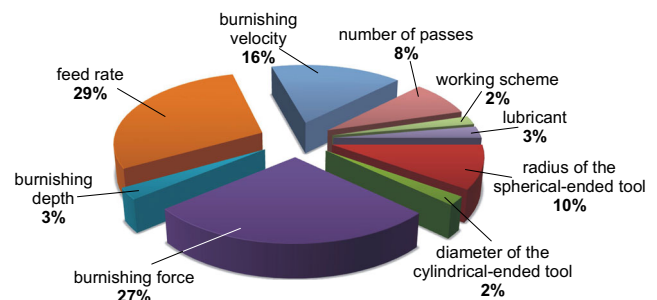


Fig. 18 Percentage share of the SB process parameters studied

5 Conclusions and directions for future investigations

Based on the analysis, the following conclusions can be made:

1. The majority of SB studies are focused on the study of SI, where the attention is focused mostly on the roughness and microhardness. Significantly less attention is paid to wear resistance and fatigue strength. The publications that examine the roughness, microhardness and residual stresses for a given material simultaneously are very few in number.
2. A very small percentage of the publications are aimed at optimizing the SB process according to the maximum fatigue strength criterion. In fact, only one publication is devoted to increasing the crack resistance of holes processed by SB.
3. The question concerning the use of SB in combination with TCD processes (for example, nitriding and cementation) is relatively weakly affected.
4. The application of SB for the treatment of holes is poorly studied.
5. The wear on the types of diamond deforming elements and the impact of that wear on the surface quality obtained have been insufficiently studied.
6. FEM is insufficiently used for a complete analysis of both the thermo-mechanical nature of the process and the effect of SB on SI.
7. The following SB governing factors are most often defined: the radius of the spherical-ended deforming element, burnishing force, feed rate, burnishing velocity and number of passes. However, experience has shown that a combination of these factors achieves a different SI results, for different workpiece diameters (10 mm versus 100 mm). The reason for these different results is the different contact area between the deforming element and the surface being treated. Therefore, another control parameter is needed to take the large-scale factor into account.
8. The sliding friction coefficient between the deforming element and the material to be treated is poorly studied.
9. Comprehensive studies comparing SB and roller/ball burnishing in terms of SI are practically absent (with the exception of Hamadache et al. [116]).
10. The possibility of processing non-metallic materials through SB has not been investigated. Recently, Babic et al. demonstrated the use of ball burnishing to process wooden components and showed that the microhardness of the surface layer increased more than seven times [121].
11. The proposed morphological matrix, which can be expanded and supplemented, is a basis for the synthesis of

new burnishing methods and tools, including those needed for special applications.

12. Based on the conclusions, the following directions for future investigations are proposed:
 - (a) Conducting extensive research to supplement the missing information in Tables 6 and 7
 - (b) Optimization of the SB process of various metals and alloys using maximum fatigue strength criterion
 - (c) Synthesis of super-hard alloys as deforming elements and the study of their wear resistance
 - (d) Study of the efficiency of SB in combination with SHT and TCD processes
 - (e) Creation of an adequate thermo-mechanical KE model with which to study the thermo-mechanical nature of SB and the effect of the SB process on SI
 - (f) Comprehensive studies comparing SB and roller/ball burnishing in terms of SI
 - (g) Investigation of the possibility of the SB of cast iron and non-metallic materials
 - (h) Synthesis of new burnishing methods and burnishing tools on the basis of the proposed morphological matrix, which can be expanded and supplemented

Funding information This work was supported by the European Regional Development Fund within the OP ‘Science and Education for Smart Growth 2014-2020’, Project CoC ‘Smart Mechatronics, Eco- and Energy Saving Systems and technologies’, No. BG05M2OP001-1.002-0023.

References

1. Griffith AA (1921) Philosophical transactions of the Royal Society of London. Series A, Containing Papers of a Mathematical or Physical Character 221:163–198
2. El-Axir MH (2002) A method of modeling residual stress distribution in turning for different materials. *Int J Mach Tools Manuf* 42(9):1055–1063
3. Sasahara H (2005) The effect on fatigue life of residual stress and surface hardness resulting from different cutting conditions of 0.45% C steel. *Int J Mach Tools Manuf* 45(2):131–136
4. Gu Y, Li H, Du B, Ding W (2019) Towards the understanding of creep-feed deep grinding of DD6 nickel-based single-crystal superalloy. *Int J Adv Manuf Technol* 100(1–4):445–455
5. Qian N, Ding W, Zhu Y (2018) Comparative investigation on grindability of K4125 and Inconel718 nickel-based superalloys. *Int J Adv Manuf Technol* 97(5–8):1649–1661
6. Daia CW, Dinga WF, Zhua YJ, Xua JH, Yu HW (2018) Grinding temperature and power consumption in high speed grinding of Inconel 718 nickel-based superalloy with a vitrified CBN wheel. *Precis Eng* 52:192–200
7. Zhou H, Ding W, Liu C (2019) Material removal mechanism of PTMCs in high-speed grinding when considering consecutive action of two abrasive grains. *Int J Adv Manuf Technol* 100(1–4): 153–165
8. Xia X, Yub T, Ding W, Xu J (2018) Grinding of Ti2AlNb intermetallics using silicon carbide and alumina abrasive wheels: tool

- surface topology effect on grinding force and ground surface quality. *Precis Eng* 53:134–145
9. Plaster HJ (1993) A tribute to Benjamin Chew Tilghman, in: proceedings of the 5th international conference on shot peening. In: pp 2–9
 10. Scibner IA (1916) Burnishing tool. United States Patent 1171146, Patented Feb. 8, 1916
 11. Ecoroll Catalogue (2006) Tools and solutions for metal surface improvement. Ecoroll Corporation Tool Technology, USA
 12. Klumpp A, Hoffmeister J, Schulze V (2014) Mechanical surface treatments, in: Conf proc 2014: ICSP-12 Goslar, Germany, pp. In: 12–24
 13. Zhuang W, Liu Q, Djugum R, Sharp PK, Paradowska A (2014) Deep surface rolling for fatigue life enhancement of laser clad aircraft aluminium alloy. *Appl Surf Sci* 320:558–562
 14. Fouad Y, Mhaede M, Wagner L (2010) Effect of mechanical surface treatment on fatigue performance of extruded ZK60 alloy. *Fatigue Fract Eng Mater Struct* 34:403–407
 15. Prevey PS, Jayaraman N, Ravintranath R (2010) Fatigue life extension of stream turbine alloys using low plasticity burnishing. Proceedings of ASME Turbo Expo 2010: Power for land, sea and air, June 14–18, 2010, Glasgow
 16. Revankar GD, Shetty R, Rao SS, Gaitonde VN (2017) Wear resistance enhancement of titanium alloy (Ti-6Al-4V) by ball burnishing process. *J Mater Resear Technol* 6(1):13–32
 17. Rajasekariah R, Vaidyanathan S (1975) Increasing the wear-resistance of steel components by ball burnishing. *Wear* 34(2): 183–188
 18. Hassan AM, Al-Dhifi SZS (1999) Improvement in the wear resistance of brass components by the ball burnishing process. *J Mater Process Technol* 96(1–3):73–80
 19. Kato H, Ueki H, Yamamoto K, Uasunaga K (2018) Wear resistance improvement by nanostructured surface layer produced by burnishing. *Mater Sci Forum* 917:231–235
 20. Krishna RM, Koorapati EP, Kotaiah R (2011) An investigation into the improvement in wear resistance of roller burnished mild steel specimen. *Int J Eng Stud* 3(2):141–148
 21. Krishna RM, Koorapati EP (2012) A study of wear resistance of non-ferrous roller burnished components. *Int J Appl Manag Sci* 3(1):11–24
 22. Rao DS, Hebbar HS, Komaraiah M, Kempaiah UN (2008) Burnishing parameters on surface hardness and wear resistance of HSLA dual-phase steels. *Mater Manuf Process* 23(3):295–302
 23. Li N, Zhao J, Xia W, Li F (2012) Fretting behaviour of burnished pure copper under oil lubricant. *Adv Mater Resear* 591(593): 1108–1112
 24. Rao DS, Hebbar HS, Komaraiah M, Kempaiah UN (2008) Investigation on the effect of ball burnishing parameters on surface roughness and corrosion resistance of HSLA dual-phase steels. *East Afric J Sci* 2(2):164–169
 25. Krishna RM, Reddy TVS (2011) Optimization of burnishing process parameters for improved corrosion resistance of aluminium and mild steel. *Int J Eng Resear Technol* 4(1):55–66
 26. Hull EH, Nerad AJ (1961) Irregular diamond burnishing tool. United States patent 2966722, patented Jan, vol 3, p 1961
 27. Prevey P (1998) Burnishing and apparatus for providing a layer of compressive residual stress in the surface of a workpiece. US Patent 5826453, Patented Oct. 27, 1998
 28. Prevey P (2002) Method and apparatus for providing a residual stress distribution in the surface of a part. US Patent 6415486, Patented Jul. 9, 2002
 29. Prevey P, Jayaraman N, Ravindranath R, Shepard M (2007) Mitigation of fretting fatigue damage in blade and disk pressure faces with LPB, ASME conference proceedings, Vol 5: Turbo Expo, May 14–17, 2007, Montreal Canada, Paper no GT 2007-27424 pp. 61–69
 30. Prevey P, Jayaraman N, Shepard M, Ware R, Cadte J, Ontko N (2008) The use of engineered compressive residual stresses to mitigate stress corrosion cracking and fatigue failure in 300M lauding gear steel. Proceeding 10th Joint FAA/DoD/NASA Aging Aircraft Conference, Palm Springs. CA
 31. Hamuiela JAG, Kuznetsov YN, Hamuiela TO (2017) Genetic-morphological synthesis of chucks. Lutsk, Veja-Druk (in Russian)
 32. Bliumberg VA, Glushtenko VF (1982) Which solution is better? Leningrad, lenizdat (in Russian)
 33. Amdouni H, Bouzaiene H, Montagne A, Nasri M, Iost A (2017) Modeling and optimization of a ball-burnishing aluminum alloy flat surface with a crossed strategy based on response surface methodology. *Int J Adv Manuf Technol* 88(1–4):801–814
 34. Bounouara A, Hamadache H, Amirat A (2018) Investigation on effect of ball burnishing on fracture toughness in spiral APIX70 pipeline steel. *Int J Adv Manuf Technol* 94(9–12):4543–4551
 35. El-Taweel TA, El-Axir MH (2009) Analysis and optimization of the ball burnishing process through the Taguchi technique. *Int J Adv Manuf Technol* 41:301–310
 36. Gharbi F, Sghaier S, Al-Fadhalah KJ, Benameur T (2011) Effect of ball burnishing process on the surface quality and microstructure properties of AISI 1010 steel plates. *J Mater Eng Perform* 20(6):903–910
 37. Nemat M, Lyons AC (2000) An investigation of the surface topography of ball burnished mild steel and aluminium. *Int J Adv Manuf Technol* 16:469–473
 38. Sarhan AAD, El-Tayeb (2014) NSM investigating the surface quality of the burnished brass C3605-fuzzy rule-based approach. *Int J Adv Manuf Technol* 71:1143–1150
 39. Travieso-Rodriges JA, Gomez-Gras G, Dessein G, Carrillo F, Alexis J, Jorba-Piero J, Aubazac N (2015) Effects of a ball-burnishing process assisted by vibrations in G10380 steel specimens. *Int J Adv Manuf Technol* 81:1757–1765
 40. Hassan AM (1997) The effects of ball- and roller-burnishing on the surface roughness and hardness of some non-ferrous metals. *J Mater Process Technol* 72:385–391
 41. Maximov JT, Duncheva GV, Amudjev IM, Krumov KK, Kuzmanov TV (2010) A new single-roller burnishing technique decreasing roughness obtained. *J Mater Sci Eng Adv Technol* 2(2):177–202
 42. Okada M, Suenobu S, Watanabe K, Yamashita Y, Asakawa N (2015) Development and burnishing characteristics of roller burnishing method with rolling and sliding effects. *Mechatronics* 29: 110–115
 43. Yatzenko VK, Zaitzev GZ, Pritchenko VF, Ivshenko LI (1985) Enhancement of load-carrying capacity of machine components by diamond burnishing. *Machinostroenie, Moscow* in Russian
 44. Korzynski M (2013) Slide diamond burnishing. In: Korzynski M (ed) *Nonconventional finishing technologies*. Polish Scientific Publishers, Warsaw, pp 9–33
 45. Konefal K, Korzynski M, Byczkowska Z, Korzynska K (2013) Improved corrosion resistance of stainless steel X6CrNiMoTi17-12-2 by slide diamond burnishing. *J Mater Process Technol* 213: 1997–2004
 46. Korzynski M, Dudek K, Kruczek B, Kocurek P (2018) Equilibrium surface texture of valve stems and burnishing method to obtain it. *Tribol Int* 124:195–199
 47. Korzynski M, Dudek K, Palczak A, Kruczek B, Kocurek P (2018) Experimental models and correlations between surface parameters after slide diamond burnishing. *Meas Sci Rev* 18(3):123–129
 48. Korzynski M, Lubas J, Swirad S, Dudek K (2011) Surface layer characteristics due to slide diamond burnishing with a cylindrical ended tool. *J Mater Process Technol* 211:84–94
 49. Korzynski M, Pacana A, Cwanek J (2009) Fatigue strength of chromium coated elements and possibility of its improvement with slide diamond burnishing. *Surf Coat Technol* 203:1670–1676

50. Korzynski M, Zarski T (2016) Slide diamond burnishing influence on surface stereometric structure of AZ91 alloy. *Surf Coat Technol* 307:590–595
51. Korzynski M (2009) A model of smoothing slide ball-burnishing and an analysis of the parameter interection. *J Mater Process Technol* 209(1):625–633
52. Korzynski M (2007) Modeling and experimental validation of force – surface roughness relation for smoothing burnishing with a spherical tool. *Int J Mach Tools Manuf* 47(12):1956–1964
53. Korzynski M (2009) Relief making on bearing sleeve surface by eccentric burnishing. *J Mater Process Technol* 209:131–138
54. Tobola D, Brostow W, Czechowski K, Rusek P, Wronska (2015) Structure and properties of burnished and nitrided AISI D2 tool steel. *Mater Sci* 21(4):511–516
55. Tobola D, Brostow W, Czechowski K, Rusek P (2017) Improvement of wear resistance of some cold working tool steels. *Wear* 382–383:29–39
56. Tobola D, Kania B (2018) Phase composition and stress state in the surface layers of burnished and gas nitrided Sverker 21 and Vanadis 6 tool steels. *Surf Coat Technol* 353:105–115
57. Tobola D, Rusek P, Czechowski K, Miller T, Duda K (2015) New indicators of burnished surface evaluation – reasons of application. *Metrologia* 52(2):263–274
58. Kuznetsov VP, Tarasov SY, Dmitriev AI (2015) Nanostructuring burnishing and subsurface shear instability. *J Mater Process Technol* 217:327–335
59. Boguslaev VA, Yatsenko VK, Yakovlev VG, Stepanova LP, Pukhalskaya GV (2008) The effect of diamond burnishing on structure and properties of detonation-gas coatings on gas-turbine engine parts. *Metal Sci Heat Treatm* 50(1–2):44–48
60. Huuki J, Laakso SVA (2013) Integrity of surface finished with ultrasonic burnishing. *Proc IMechE Part B: J Eng Manuf* 227(1):45–53
61. Huuki J, Laakso SVA (2017) Surface improvement of shafts by the diamond burnishing and ultrasonic burnishing techniques. *Int J Mach Machinabil Mater* 19(3):246–258
62. Liska J, Liska K, Kodacsy J (2014) Hard cutting and diamond burnishing of 100Cr6 steel bearings. *Key Eng Mater* 581:169–175
63. Liska K, Kodacsy J, Liska J (2013) Investigation of microgeometry on diamond burnished surfaces. In: 8th research/expert conference with international participations “quality 2013”, Neum, June 06–08, 2013, pp. pp 615–620
64. Luo H, Liu J, Wang L, Zhong Q (2006) Study of the mechanism of the burnishing process with cylindrical polycrystalline diamond tools. *J Mater Process Technol* 180(1–3):9–16
65. Luo H, Liu J, Wang L, Zhong Q (2006) The effect of burnishing parameters on burnishing force and surface microhardness. *Int J Adv Manuf Technol* 28(7–8):707–713
66. Luo H, Liu J, Zhong Q (2005) Investigation of the burnishing process with PCD tool on non-ferrous metals. *Int J Adv Manuf Technol* 25(5–6):454–459
67. Luo H, Wang L, Zhang C (2001) Study on the aluminum alloy burnishing processing and the existence of the outstripping phenomenon. *J Mater Process Technol* 116(1):88–90
68. Sachin B, Narendranath S, Chakradhar D (2018) Effect of cryogenic diamond burnishing on residual stress and microhardness of 17 – 4 PH stainless steel. *Mater Today* 5(9) Part 3:18393–18399
69. Sachin B, Narendranath S, Chakradhar D (2018) Experimental evaluation of diamond burnishing for sustainable manufacturing. *Mater Res Express* 5(10):106514
70. Sachin B, Narendranath S, Chakradhar D (2019) Sustainable diamond burnishing of 17-4 PH stainless steel for enhanced surface integrity and product performance by using a novel modified tool. *Mater Res Express* 6:046501
71. Maximov JT, Duncheva GV, Anchev AP, Dunchev VP (2019) Crack resistance enhancement of joint bar holes by slide diamond burnishing using new tool equipment. *Int J Adv Manuf Technol*. <https://doi.org/10.1007/s00170-019-03405-x>
72. Maximov JT, Duncheva GV (2012) Finite element analysis and optimization of spherical motion burnishing of low-alloy steel. *Proc. IMechE, Part C: J Mech Eng Sci* 226(1):161–176
73. Maximov JT, Duncheva GV, Amudjev IM, Kuzmanov TV (2012) Modelling the power parameters of the spherical motion burnishing. *Proc IMechE, Part C: J Mech Eng Sci* 226(2):498–510
74. Maximov JT, Anchev AP, Duncheva GV, Ganev N, Selimov KF (2017) Influence of the process parameters on the surface roughness, micro-hardness, and residual stresses in slide burnishing of high-strength aluminum alloys. *J Braz Soc Mech Sci Eng* 39(8):3067–3078
75. Maximov JT, Duncheva GV, Anchev AP, Amudjev IM, Kuzmanov VT (2014) Enhancement of fatigue life of rail-end-bolt holes by slide diamond burnishing. *Eng Solid Mech* 2(4):247–264
76. Maximov JT, Anchev AP, Dunchev VP, Ganev N, Duncheva GV, Selimov KF (2017) Effect of slide burnishing basic parameters on fatigue performance of 2024-T3 high-strength aluminium alloy. *Fatigue Fract Eng Mater Struct* 40(11):1893–1904
77. Maximov JT, Anchev AP, Duncheva GV, Ganev N, Selimov KF, Dunchev VP (2019) Impact of slide diamond burnishing additional parameters on fatigue behaviour of 2024-T3 Al alloy. *Fatigue Fract Eng Mater Struct* 42(1):363–373
78. Maximov JT, Anchev AP, Duncheva GV (2015) Modeling of the friction in tool-workpiece system in diamond burnishing process. *Coupled Syst Mech* 4(4):279–295
79. Maximov JT, Kuzmanov TV, Duncheva GV, Ganev N (2009) Spherical motion burnishing implemented on lathes. *Int J Mach Tools Manuf* 49:824–831
80. Maximov JT, Duncheva GV, Anchev AP, Ganev N, Amudjev IM, Dunchev VP (2018) Effect of slide burnishing method on the surface integrity of AISI 316Ti chromium-nickel steel. *J Braz Soc Mech Sci Eng* 40(194). <https://doi.org/10.1007/s40430-018-1135-3>
81. Maximov JT (2013) Spherical motion burnishing. In: Korzynski M (ed) *Nonconventional finishing technologies*. Polish Scientific Publishers, Warsaw, pp 35–59
82. Maximov JT, Duncheva GV, Anchev AP (2019) A temperature-dependent, non-linear kinematic/isotropic hardening material constitutive model of the surface layer of 37Cr4 steel subjected to slide burnishing. *Arab J Sci Eng*. <https://doi.org/10.1007/s13369-019-03765-2>
83. Maximov JT, Duncheva GV, Anchev AP, Ganev N, Dunchev VP (2019) Effect of cyclic loading on fatigue performance of slide burnishing components made of low-alloy medium carbon steel. *Fatigue Fract Eng Mater Struct* 42:1414–1425. <https://doi.org/10.1111/ffe.13001>
84. Aliev KT, Aslanov TI (1979) The influence of diamond burnishing on the fatigue strength and wear resistance of the shafts of petroleum chains. *Chem Pet Eng* 15(6):459–461
85. Bednarski P, Bialo D, Brostow W, Czechowski K, Polowski W, Rusek P, Tobola D (2013) Improvement of tribological properties of matrix composites by means of slide burnishing. *Mater Sci* 19(4):367–372
86. Iwamoto T, Tanaka H, Yanagi K (2011) An experimental study on diamond burnishing tool Wear and its lifetime estimation. In: *Proceedings of the international conference on Technology of Plasticity ICTP'2011, Aachen, 2011*, pp 82–86
87. Lin YC, Wang SW, Lai HY (2004) The relationship between surface roughness and burnishing factor in the burnishing process. *Int J Adv Manuf Technol* 23(9–10):666–671
88. Labanowski J, Ossowska A (2006) Influence of burnishing on stress corrosion cracking susceptibility of duplex steel. *J Achiev Mater Manuf Eng* 19(1):46–52

89. Nestler A, Schubert A (2015) Effect of machining parameters on surface properties in slide diamond burnishing of aluminium matrix composites. *Materials Today: Proceedings* 2S:S156–S161
90. Okada M, Shinya M, Matsubara H, Kozuka H, Tachiya H, Asakawa N, Otsu M (2017) Development and characterization of diamond tip burnishing with a rotary tool. *J Mater Process Technol* 244:106–115
91. Okada M, Terada S, Miura T, Iwai Y, Takazawa T, Kataoka Y, Kihara T, Otsu M (2018) Fundamental burnishing characteristics of Ni-based alloy using coated carbide tool. *Proc Manuf* 15:1278–1283
92. Pa PS (2010) Continuous finishing processes using a combination of burnishing and electrochemical finishing on bore surface. *Int J Adv Manuf Technol* 49:147–154
93. Pang C, Luo H, Zhang Z, Ma Y (2018) Precipitation behavior and grain refinement of burnishing Al-Zn-mg alloy. *Progress Nat Sci Mater Int* 28:54–59
94. Radziejewska J, Skrzypek S (2009) Microstructure and residual stresses in surface layer of simultaneously laser alloyed and burnished steel. *J Mater Process Technol* 209:2047–2056
95. Saldana-Robles A, Plascencia-Mora H, Aguilera-Gomez E, Saldana-Robles A, Marquez-Herrera A, Diosdado-De la Pena JA (2018) Influence of ball-burnishing on roughness, hardness and corrosion resistance of AISI 1045 steel. *Surf Coat Technol* 339:191–198
96. Shiou FJ, Banh QN (2016) Development of an innovative small ball-burnishing tool embedded with a load cell. *Int J Adv Manuf Technol* 87(1–4):31–41
97. Shiou FJ, Chen CH (2003) Determination of optimal ball-burnishing parameters for plastic injection moulding steel. *Int J Adv Manuf Technol* 21(3):177–185
98. Shiou FJ, Huang SJ, Shin AJ, Zhu J, Yoshino M (2017) Fine surface finish of a hardened stainless steel using a new burnishing tool. *Procedia Manuf* 10:208–217
99. Shvetsov AN, Skuratov DL (2017) Evolution of the residual stresses formation from FeCo.15Cr12Ni2 steel in the part surface during the diamond smoothing. *Procedia Eng* 176:355–362
100. Shvetsov AN, Skuratov DL (2017) Surface microgeometry of structural-steel samples after diamond burnishing. *Russ Eng Res* 37(6):536–538
101. Swirad S (2007) The effect of burnishing parameters on steel fatigue strength. *Nonconventional Technol Rev* 1:113–118
102. Swirad S (2011) The surface texture analysis after slide burnishing with cylindrical elements. *Wear* 271:576–581
103. Szutkowska M, Tobola D, Czechowski K (2015) Burnishing of aluminium alloy surface using diamond matrix composite tools. *Key Eng Mater* 641:39–46
104. Tanaka H, Ishii W, Yanagi K (2011) Optimal burnishing conditions and mechanical properties of surface layer by surface modification effect induced of applying burnishing process to stainless steel and aluminum alloy. *J Jpn Soc Technol Plast* 52(605):726–730 in Japanese
105. Tanaka H, Nishinaka K, Yanagi K (2012) Development of hydraulic burnishing tool for discontinuous surface finishing – machining characteristics of hydrostatic burnishing tool with single crystal diamond tip. *J Jpn Soc Technol Plast* 53(621):924–928 in Japanese
106. Tanaka H, Tabuto H, Yanagi K, Futamura M (2009) Effect of surface hardened steel texture of preliminary process on burnishing process – a metrological study of hardened steel surface finishing using diamond burnishing tool. *J Jpn Soc Technol Plast* 50(581):555–559 in Japanese
107. Teimouri R, Amini S, Bami AB (2018) Evaluation of optimized surface properties and residual stress in ultrasonic assisted ball burnishing of AA6061-T6. *Measurement* 116:129–139
108. Varga G, Ferencsik V (2018) Investigation of the influence of different burnishing parameters on shape correctness and residual stresses. *IOP Conf Series: Mater Sci Eng* 448:012016. <https://doi.org/10.1088/1757-899X/448/1/012016>
109. Yu X, Wang L (1999) Effect of various parameters on the surface roughness of an aluminium alloy burnished with a spherical surfaced polycrystalline diamond tool. *Int J Mach Tools Manuf* 39(3): 459–469
110. Brostow W, Czechowski K, Polowski W, Rusek P, Tobola D, Wronska I (2013) Slide diamond burnishing of tool steels with adhesive coatings and diffusion layers. *Mater Res Innov* 17(4): 269–277
111. Brostow W, Lohse S, Osmanson A, Tobola D (2018) Mechanical finishing and ion beams application to cold working tool steels: consequences for scratch resistance. *Mater Res Soc Commun* 8(1): 178–182
112. Buldum BB, Cagan SC (2018) Study of ball burnishing process on the surface roughness and microhardness of AZ91D alloy. *Exp Tech* 42(2):233–241
113. Czechowski K, Tobola D (2017) Slide finishing burnishing of metal alloys and metal matrix composites. *Mechanik NR* (7):1–3
114. Esme U (2010) Use of grey based Taguchi method in ball burnishing process for the optimization of surface burnishing and microhardness of AA7075 aluminium alloy. *Mater Technol* 44:129–135
115. Gharbi F, Sghaier S, Hamdi H, Benameur T (2012) Ductility improvement of aluminum 1050A rolled sheet by a newly designed ball burnishing tool device. *Int J Adv Manuf Technol* 60(1–4):87–99
116. Hamadache H, Laouar L, Zeghib NE, Chaoui K (2006) Characteristics of Rb40 steel superficial layer under ball and roller burnishing. *J Mater Process Technol* 180(1–3):130–136
117. Hamadache H, Zemouri Z, Laouar L, Dominiak S (2014) Improvement of surface conditions of 36CrNiMo6 steel by ball burnishing process. *J Mech Sci Technol* 28(4):1491–1498
118. Hankare AV, Sapkal AA, Dounde AA (2017) Effect of diamond burnishing process on surface roughness of AISI 4140 alloy steel. *J Adv Sci Technol* 13(1):405–410
119. He D, Wang B, Zhang J, liao S, Deng WJ (2018) Investigation of interference effect on the burnishing process. *Int J Adv Manuf Technol* 95:1–10
120. Maximov JT, Dunchewa GV, Anchev AP (2017) Fatigue Life Increase of 2024-T3 Aluminium Alloy by Slide Burnishing. LAP Lambert Academic Publishing, Saarbrücken
121. Babic M, Kocovic V, Vukelic D, Mihajlovic G, Eric M, Tadic B (2017) Investigation of ball burnishing processing on mechanical characteristics of wooden elements. *Proc IMechE Part C: J Mech Eng Sci* 231(1):120–127

Publisher's note Springer Nature remains neutral with regard to jurisdictional claims in published maps and institutional affiliations.